

## Nonlinear exciton transfer in protein helices

This article has been downloaded from IOPscience. Please scroll down to see the full text article.

2003 J. Phys.: Condens. Matter 15 441

(<http://iopscience.iop.org/0953-8984/15/3/309>)

View [the table of contents for this issue](#), or go to the [journal homepage](#) for more

Download details:

IP Address: 171.66.16.119

The article was downloaded on 19/05/2010 at 06:29

Please note that [terms and conditions apply](#).

# Nonlinear exciton transfer in protein helices

**S Komarnicki and D Hennig**

Freie Universität Berlin, Fachbereich Physik, Institut für Theoretische Physik, Arnimallee 14,  
D-14195 Berlin, Germany

Received 4 July 2002

Published 13 January 2003

Online at [stacks.iop.org/JPhysCM/15/441](http://stacks.iop.org/JPhysCM/15/441)

## Abstract

We study the transfer of vibronic excitation energy in helical forms of proteins. The steric structure of the helix protein is modelled by a three-dimensional network of oscillators representing peptide groups. The covalent and hydrogen bonds between the peptide groups are described by pair interaction potentials. Each peptide group possesses one internal vibrational (excitonic) degree of freedom embodying the amide-I mode. The transfer dynamics of an amide-I exciton along the helix is expressed in terms of a tight-binding system. In the first part of this paper we study a reduced system arising when the vibrations of the covalent bonds are neglected. For the resulting system consisting of the exciton coupled to the hydrogen bond vibrations oriented along the helix axis we construct polaron solutions. Subsequently we investigate the mobility of the polarons within the complete protein matrix including deformations of the covalent bonds too. In particular we show that, during a phase of adaptation going along with internal energy exchange between the exciton and the bond vibrations, a relaxation into a new steady regime takes place. The newly reached equilibrium state is characterized by a localized exciton breather and is attributed local deformations of the steric peptide cage in the form of phonobreathers. Finally, coherent motion of an exciton breather is initiated through suitable injection of kinetic energy. In this way the long-range transfer of vibronic amide-I energy in the steric protein cage is provided. Interestingly, the  $\alpha$ -helix possesses better facilities in supporting mobile localized excitons compared to the 3–10-helix form of proteins.

## 1. Introduction

The transfer of vibrational energy within proteins proceeds over remarkably long ranges and with astonishing efficiency. For a theoretical description of the energy storage and transfer processes in proteins Davydov and co-workers [1] were among the first to invoke ideas from the theory of polarons. For the investigation of the energy transfer in the protein  $\alpha$ -helix form, as the most common secondary structure of proteins, Davydov considered three strands of hydrogen bonded peptide units of an  $\alpha$ -helix which form paths for the energy transfer along

the helix backbone [2]. Apart from a few studies of the original three-strand Davydov model [2–6] most works were based on one-dimensional reductions of the three-dimensional structure of the  $\alpha$ -helix proteins for which only one of the three strands was taken into account for the energy transfer. The molecular structure of such a single hydrogen bonded polypeptide chain is described by a simple one-dimensional lattice model (the one-strand Davydov system) and the excitation energy propagation is described with the help of the exciton formalism. The storage mechanism relies on the nonlinear interaction between the intra-peptide vibronic (amide-I quantum) exciton and the acoustic phonons of the polypeptide chain (deformation of the hydrogen bonds) which creates a polaronic compound of self-trapped vibronic amide-I energy together with its local deformation of the protein backbone. This polaron can travel as a moving pulse in the form of a solitary wave along a strand of the  $\alpha$ -helix. The one-strand Davydov system has been extensively studied (see e.g. [3–20]). Recently pump–probe experiments performed with myoglobin (an almost entirely  $\alpha$ -helix in its secondary structure) [21] and acetanilide (as a molecular crystal with hydrogen bonded chains of peptide units) [22, 23] exhibit an anharmonic response in the amide I band indicating the generation of nonlinear excitations which supports the Davydov model.

Real biomolecules are three-dimensional objects [24, 25]. (Studies concerning polaronic and/or solitonic energy and particle transfer in two- and three-dimensional models of biomolecules going beyond one-dimensional polypeptide chain models can be found in [26–31].) In fact, as far as the helical proteins are concerned, not only longitudinal deformations along a strand of hydrogen bonded peptide units influence the excitonic transfer behaviour but also genuine steric vibrations of the peptide units within the protein matrix, leading to more complex structural deformations. The three-strand Davydov model for the  $\alpha$ -helix protein already incorporates aspects of the steric structure of the protein matrix involving, besides the interaction between the vibrations of the hydrogen bridges and the exciton, also the coupling between the latter and the covalent bond vibrations. The findings in [3, 4, 6, 32] suggest that incorporation of all three strands into the dynamical studies of energy transfer in  $\alpha$ -helix proteins is of importance for the transfer features.

The aim of the present paper is to generalize the ideas presented in a previous article [32] where the transfer of vibronic energy within the steric cage of a protein helix has been discussed using the three-strand Davydov model. For simulation of the energy storage and transport we have applied recent developments in polaron dynamics such as the construction of exact polaron states and the initiation of their motion through suitable excitations of certain normal modes [33, 34]. The study of the three-strand Davydov model in [32] demonstrated that the exciton motion in the protein matrix takes place along the hydrogen pathway and the covalent channel is suppressed. However, the too simplified couplings of the bond deformations to the exciton motion should be regarded with more criticism. Moreover, in the context of the three-strand Davydov model the rest positions of the peptide units are situated on the surface of a cylinder mimicking the helical shape. The deformations of the hydrogen and covalent bonds, respectively are assumed to be linked with merely one-dimensional displacements of the peptide units oriented along the axis respectively the radius of this cylinder [2]. In particular, the deformations of the hydrogen and covalent bonds proceed independent of each other, i.e. they are effectively decoupled. However, it is rather so that any distortion of a peptide unit from its rest position leads inevitably to simultaneous deformations of the adjacent covalent as well as hydrogen bonds. Therefore, we extend the three-strand Davydov model in the way that we allow each peptide unit to genuinely fulfil individual motions in all three dimensions, with the consequence that the local steric deformations of the peptide cage influence the excitonic parameters and thus the excitonic transfer. There arises at least two questions, namely, whether with regard to the polaronic energy storage mechanism the interplay between the genuine three-

dimensional deformations of the protein cage and the exciton still results in the formation of polaron solutions reminiscent of the ones occurring in the three-strand Davydov model. In addition, is it still possible to achieve coherent exciton transfer within the rather complicated dynamics of the three-dimensional protein cage analogous to the energy transfer mediated by mobile polarons in the simpler one (respectively three-strand system) considered in [32]? In the current paper these problems will be addressed and we organize our paper then as follows. In the first part we discard the vibrations of the covalent bonds and investigate the dynamics of the resulting simplified system consisting of the exciton coupled to the hydrogen bond vibrations oriented along the helix axis with a view to polaron solutions. The latter are constructed exactly with the help of a nonlinear map method. Subsequently we investigate the stability of the polarons within the vibrational system of the full protein matrix including deformations of the covalent bonds too. In particular we show that, during a phase of adaptation going along with internal energy exchange between the exciton and the bond vibrations, a relaxation into a new steady regime takes place. The new equilibrium state reached is characterized by a localized exciton and attributed to local deformations of the steric peptide cage in the form of breathers. We attempt to initiate coherent motion of such an exciton breather and pay special interest to the impact of the different helix geometries ( $\alpha$ -helix and 3–10-helix) on the breather mobility. Finally we summarize our results.

## 2. Steric helix protein model

The most common secondary structure of proteins develops from polypeptide chains folded in the form of a helix. To this end the primary structure of the one-dimensional sequence of covalently linked peptide groups gets tightly curled about its longitudinal axis. The resulting three-dimensional secondary structure is stabilized by hydrogen bonds formed between the carbonyl oxygen of a peptide unit  $n$  and the amide hydrogen of a peptide unit  $n+m$  resulting in  $m$  longitudinal strands of H-bonded peptide groups [24, 25]. In our model approach the peptide groups are treated as mass entities incorporated in a three-dimensional network modelling the helix structure of the protein matrix. The covalent and hydrogen bonds between the peptide units are described through point–point interaction potentials. For each peptide unit one internal excitonic degree of freedom represented by the C=O stretching (amide-I) mode is taken into account. Our Hamiltonian modelling the transfer of vibronic amide-I energy in helix proteins comprises then of two parts:

$$H = H_{exc} + H_{vib}, \quad (1)$$

with  $H_{exc}$  as the contribution from the local amide-I excitation of a peptide group and  $H_{vib}$  describes the dynamics of the bond vibrations of the protein matrix. The excitonic part is expressed in terms of a tight-binding system:

$$H_{exc} = \sum_{n,\mu} \{ \epsilon_{n,\mu} |c_{n,\mu}|^2 - J_{n+1,n}^\mu [c_{n+1,\mu}^* c_{n,\mu} + c_{n+1,\mu} c_{n,\mu}^*] + L_{\mu+1,\mu}^n [c_{n,\mu+1}^* c_{n,\mu} + c_{n,\mu+1} c_{n,\mu}^*] \}. \quad (2)$$

The index  $n$  denotes the site on a strand of hydrogen bonded peptide groups while the covalently linked strands are labelled by the strand index  $\mu$ . The complex amplitude  $c_{n,\mu}$  determines the probability of the exciton (a quantum of the amide-I energy) to occupy the peptide group at the site  $(n, \mu)$ .  $\epsilon_{n,\mu}$  is the local amide-I vibronic energy,  $J_{n+1,n}^\mu$  is the transfer matrix element arising through dipole–dipole interaction which is responsible for the transfer of the amide-I vibronic energy between neighbouring peptide groups of a single hydrogen bonded strand and  $L_{\mu+1,\mu}^n$  is

the inter-strand transfer matrix element accomplishing the transfer between covalently linked peptide groups of different strands.

The peptide groups as the constituents of the protein matrix are treated as rigid mass points being able to move in three dimensions. The arrangements of the peptide groups within the sterical geometry of the helical protein matrix is conveniently described in a cylindrical coordinate frame whose  $z$  axis coincides with the helix axis and the coordinates of the rest positions of the peptide groups are determined by

$$x_{n,\mu}^0 = r \cos[2\pi L/l(3n + \mu)], \quad (3)$$

$$y_{n,\mu}^0 = r \sin[2\pi L/l(3n + \mu)], \quad (4)$$

$$z_{n,\mu}^0 = (3n + \mu)l, \quad (5)$$

with the distance  $l$  between two neighbouring peptide groups situated at sites  $(n, \mu)$  and  $(n, \mu \pm 1)$ .  $r$  is the radius of the cylinder spanning the helix and  $L$  is the step size of the helix. The winding ratio  $l/L = 3$  determines the number of peptide groups per single loop of the helix.

Covalent bonds are formed between nearest-neighbouring units at  $(n, \mu)$  and  $(n, \mu \pm 1)$  of the primary structure and the peptide groups situated at  $(n, \mu)$  and  $(n, \pm 1\mu)$  are linked through hydrogen bonds. In the case of the  $\alpha$ -helix (3–10-helix) two peptide groups being four (three) sites apart from each other in the primary structure of the one-dimensional polypeptide chain are linked through a hydrogen bond resulting in four (three) strands of the helix. For an illustration of the steric protein matrix models see [31].

Due to the fact that the strong covalent bonds (with bond energies of the order of 50–250 kcal mol<sup>-1</sup>) are considerably more rigid than the rather weak and flexible H-bonds (with bond energies 1–7 kcal mol<sup>-1</sup>) [24] it is appropriate to model the rather small-amplitude vibrations of the covalent bonds in a harmonic fashion. The anharmonic vibrational dynamics of the elastic hydrogen bonds evolves in Morse potentials. The Hamiltonian of the intermolecular vibrational dynamics of the protein matrix is given by

$$\begin{aligned} H_{inter} &= \frac{1}{2m} \sum_n \sum_\mu p_{n,\mu}^2 + \sum_n \sum_\mu U_{cov}(r_{n,\mu}) + U_{hyd}(s_{n,\mu}) \\ &= \frac{1}{2m} \sum_n \sum_\mu p_{n,\mu}^2 + \frac{1}{2}\kappa \sum_n \sum_\mu r_{n,\mu}^2 + D \sum_n \sum_\mu (1 - \exp[-as_{n,\mu}])^2, \end{aligned} \quad (6)$$

with the momentum vector  $p_{n,\mu} = (p_{n,\mu}^{(x)}, p_{n,\mu}^{(y)}, p_{n,\mu}^{(z)})$  associated with the displacements  $(x_{n,\mu}, y_{n,\mu}, z_{n,\mu})$  of the peptide units from their rest positions  $(x_{n,\mu}^{(0)}, y_{n,\mu}^{(0)}, z_{n,\mu}^{(0)})$ . The deviations of the covalent and hydrogen bond lengths from their rest lengths  $r_{n,\mu}^{(0)} = \sqrt{(\Delta x_\mu^{(0)})^2 + (\Delta y_\mu^{(0)})^2 + (\Delta z_\mu^{(0)})^2}$  and  $s_{n,\mu}^{(0)} = \sqrt{(\Delta x_n^{(0)})^2 + (\Delta y_n^{(0)})^2 + (\Delta z_n^{(0)})^2}$ , respectively, are expressed as

$$\begin{aligned} r_{n,\mu} &= [(x_{n,\mu} - x_{n,\mu-1} + \Delta x_\mu^{(0)})^2 + (y_{n,\mu} - y_{n,\mu-1} + \Delta y_\mu^{(0)})^2 \\ &\quad + (z_{n,\mu} - z_{n,\mu-1} + \Delta z_\mu^{(0)})^2]^{1/2} - r_{n,\mu}^{(0)}, \end{aligned} \quad (7)$$

$$\begin{aligned} s_{n,\mu} &= [(x_{n,\mu} - x_{n-1,\mu} + \Delta x_n^{(0)})^2 + (y_{n,\mu} - y_{n-1,\mu} + \Delta y_n^{(0)})^2 \\ &\quad + (z_{n-1,\mu} - z_{n,\mu} + \Delta z_n^{(0)})^2]^{1/2} - s_{n,\mu}^{(0)}, \end{aligned} \quad (8)$$

with the abbreviations  $\Delta x_\mu^{(0)} = x_{n,\mu}^{(0)} - x_{n,\mu-1}^{(0)}$ ,  $\Delta y_\mu^{(0)} = y_{n,\mu}^{(0)} - y_{n,\mu-1}^{(0)}$ ,  $\Delta z_\mu^{(0)} = z_{n,\mu}^{(0)} - z_{n,\mu-1}^{(0)}$ ,  $\Delta x_n^{(0)} = x_{n,\mu}^{(0)} - x_{n-1,\mu}^{(0)}$ ,  $\Delta y_n^{(0)} = y_{n,\mu}^{(0)} - y_{n-1,\mu}^{(0)}$  and  $\Delta z_n^{(0)} = z_{n,\mu}^{(0)} - z_{n-1,\mu}^{(0)}$ . The parameter  $\kappa$  regulates the stiffness of the covalent bond chain,  $m$  is the mass of a single peptide unit,  $D$  determines the break-up energy of the hydrogen bond and  $a$  is the range parameter of

the Morse potential. The point–point intermolecular interaction potentials are normalized as  $U_{cov}(r_{n,\mu}^{(0)}) = U_{hyd}(s_{n,\mu}^{(0)}) = 0$  and  $U'_{cov}(r_{n,\mu}^{(0)}) = U'_{hyd}(s_{n,\mu}^{(0)}) = 0$ .

The coupling between the excitonic degree of freedom and the bond vibrations stems from a dynamical dependence of the excitonic parameters on the covalent (hydrogen) bond lengths  $r_{n,\mu}$  ( $s_{n,\mu}$ ) in the following fashion:

$$\epsilon_{n,\mu} = \epsilon_0 + \alpha_c(r_{n,\mu+1} + r_{n,\mu}) + \alpha_h(s_{n+1,\mu} + s_{n,\mu}), \quad (9)$$

$$J_{n+1,n}^\mu = J_0 + \beta_h s_{n+1,\mu}, \quad (10)$$

and

$$L_{\mu+1,\mu}^n = L_0 + \beta_c r_{n,\mu+1}, \quad (11)$$

with the coupling parameters  $\alpha_c$ ,  $\alpha_h$ ,  $\beta_c$  and  $\beta_h$ . The values of the parameters for the transfer of vibronic energy contained in the amide-I mode of helix proteins are given by [1, 5, 11]  $\epsilon_0 = 0.205$  eV,  $J_0 = 1.55 \times 10^{-22}$  N m,  $L_0 = 2.46 \times 10^{-22}$  N m,  $\alpha_h = (2-6) \times 10^{-11}$  N,  $2a^2D = (13.0-19.5)$  N m $^{-1}$ ,  $\beta_h = 7.21 \times 10^{-13}$  N and  $m = 5, 7 \times 10^{-25}$  kg. As far as the values of  $\alpha_c$ ,  $\beta_c$  and  $\kappa$  are concerned we note that there exist no reliable data from experiments and we treat them as adjustable parameters. The geometry of the  $\alpha$ -helix (3–10-helix) is determined by a pitch (height of one turn of the helix) of 5.4 Å (6 Å), distance  $l = 1.5$  Å ( $l = 2.0$  Å) and radius  $r = 2.8$  Å ( $r = 3.0$  Å).

For the forthcoming studies we introduce the dimensionless time  $t \rightarrow (J_0/\hbar)t$  and use accordingly the scaled quantities:

$$\tilde{x}_{n,\mu} = \sqrt{\frac{J_0 m}{\hbar^2}} x_{n,\mu}, \quad \tilde{a} = \sqrt{\frac{\hbar^2}{J_0 m}} a, \quad (12)$$

$$\tilde{\alpha} = \frac{\hbar}{\sqrt{m} J_0^{3/2}} \alpha, \quad \tilde{\kappa} = \frac{\hbar^2}{J_0^2 m} \kappa, \quad (13)$$

$$\tilde{p}_{n,\mu}^{(x)} = \frac{1}{\sqrt{m} J_0} p_{n,\mu}^{(x)}, \quad \tilde{D} = \frac{D}{J_0}, \quad \tilde{L} = \frac{L_0}{J_0}. \quad (14)$$

The values of the scaled parameters are given by  $J_0 = 1$ ,  $L_0 = 1.587$ ,  $\alpha_h = (1.447-4.342)$ ,  $2a^2D = (10.554-15.832)$  and  $\beta_h = 0.072$ . The remaining parameters are estimated as follows:  $\alpha_c = 0.5$ ,  $\beta_c = 0.01$  and  $\kappa = 25$ .

The system of coupled equations of motion is determined as

$$i\dot{c}_{n,\mu} = \frac{\partial H}{\partial c_{n,\mu}^*}, \quad (15)$$

$$\dot{p}_{n,\mu}^{(x)} = -\frac{\partial H}{\partial x_{n,\mu}}, \quad \dot{x}_{n,\mu} = \frac{\partial H}{\partial p_{n,\mu}^{(x)}}, \quad (16)$$

$$\dot{p}_{n,\mu}^{(y)} = -\frac{\partial H}{\partial y_{n,\mu}}, \quad \dot{y}_{n,\mu} = \frac{\partial H}{\partial p_{n,\mu}^{(y)}}, \quad (17)$$

$$\dot{p}_{n,\mu}^{(z)} = -\frac{\partial H}{\partial z_{n,\mu}}, \quad \dot{z}_{n,\mu} = \frac{\partial H}{\partial p_{n,\mu}^{(z)}} \quad (18)$$

and is explicitly

$$i \frac{dc_{n,\mu}}{dt} = \epsilon_{n,\mu} c_{n,\mu} - J_{n+1,n}^\mu c_{n+1,\mu} - J_{n,n-1}^\mu c_{n-1,\mu} + L_{\mu+1,\mu}^n c_{n,\mu+1} + L_{\mu,\mu-1}^n c_{n,\mu-1} \quad (19)$$

$$\begin{aligned}
\frac{dp_{n,\mu}^{(x)}}{dt} = & \alpha_c \left( |c_{n,\mu-1}|^2 \frac{(x_{n,\mu} - x_{n,\mu-1} + \Delta x_\mu^0)}{r_{n,\mu} + r_{n,\mu}^0} + |c_{n,\mu}|^2 \left[ \frac{(x_{n,\mu} - x_{n,\mu-1} + \Delta x_\mu^0)}{r_{n,\mu} + r_{n,\mu}^0} \right. \right. \\
& \left. \left. - \frac{(x_{n,\mu+1} - x_{n,\mu} + \Delta x_{\mu+1}^0)}{r_{n,\mu+1} + r_{n,\mu+1}^0} \right] - |c_{n,\mu+1}|^2 \frac{(x_{n,\mu+1} - x_{n,\mu} + \Delta x_{\mu+1}^0)}{r_{n,\mu+1} + r_{n,\mu+1}^0} \right) \\
& + \alpha_h \left( |c_{n-1,\mu}|^2 \frac{(x_{n,\mu} - x_{n-1,\mu} + \Delta x_n^0)}{s_{n,\mu} + s_{n,\mu}^0} + |c_{n,\mu}|^2 \left[ \frac{(x_{n,\mu} - x_{n-1,\mu} + \Delta x_n^0)}{s_{n,\mu} + s_{n,\mu}^0} \right. \right. \\
& \left. \left. - \frac{(x_{n+1,\mu} - x_{n,\mu} + \Delta x_{n+1}^0)}{s_{n+1,\mu} + s_{n+1,\mu}^0} \right] - |c_{n+1,\mu}|^2 \frac{(x_{n+1,\mu} - x_{n,\mu} + \Delta x_{n+1}^0)}{s_{n+1,\mu} + s_{n+1,\mu}^0} \right) \\
& - \beta_h \frac{(x_{n,\mu} - x_{n-1,\mu} + \Delta x_n^0)}{s_{n,\mu} + s_{n,\mu}^0} [c_{n,\mu}^* c_{n-1,\mu} + c_{n,\mu} c_{n-1,\mu}^*] \\
& + \beta_h \frac{(x_{n+1,\mu} - x_{n,\mu} + \Delta x_{n+1}^0)}{s_{n+1,\mu} + s_{n+1,\mu}^0} [c_{n+1,\mu}^* c_{n,\mu} + c_{n+1,\mu} c_{n,\mu}^*] \\
& + \beta_c \frac{(x_{n,\mu} - x_{n,\mu-1} + \Delta x_\mu^0)}{r_{n,\mu} + r_{n,\mu}^0} [c_{n,\mu}^* c_{n,\mu-1} + c_{n,\mu} c_{n,\mu-1}^*] \\
& - \beta_c \frac{(x_{n,\mu+1} - x_{n,\mu} + \Delta x_{\mu+1}^0)}{r_{n,\mu+1} + r_{n,\mu+1}^0} [c_{n,\mu+1}^* c_{n,\mu} + c_{n,\mu+1} c_{n,\mu}^*] \\
& + \kappa \left( r_{n,\mu} \frac{(x_{n,\mu} - x_{n,\mu-1} + \Delta x_\mu^0)}{r_{n,\mu} + r_{n,\mu}^0} - r_{n,\mu+1} \frac{(x_{n,\mu+1} - x_{n,\mu} + \Delta x_{\mu+1}^0)}{r_{n,\mu+1} + r_{n,\mu+1}^0} \right) \\
& + 2aD \left( [1 - e^{-as_{n,\mu}}] e^{-as_{n,\mu}} \frac{(x_{n,\mu} - x_{n-1,\mu} + \Delta x_n^0)}{s_{n,\mu} + s_{n,\mu}^0} \right. \\
& \left. - [1 - e^{-as_{n+1,\mu}}] e^{-as_{n+1,\mu}} \frac{(x_{n+1,\mu} - x_{n,\mu} + \Delta x_{n+1}^0)}{s_{n+1,\mu} + s_{n+1,\mu}^0} \right) \tag{20}
\end{aligned}$$

$$\frac{dx_{n,\mu}}{dt} = \frac{p_{n,\mu}^{(x)}}{m}, \tag{21}$$

where we omitted the tildes for simpler notation.

Correspondingly, the equations for the  $y$  and  $z$  components are obtained by substituting  $x \rightarrow y, z$  in equations (20) and (21), respectively. For later use we state that the system of equations (19)–(21) is referred to as the *full* system.

### 3. Polaron solutions

For the discussion of a nonlinear mechanism for the energy transfer in helical proteins we focus, as a first step, our interest on the construction of (standing) polaron solutions consisting of an localized exciton and its attributed local lattice deformation. Subsequently, we attempt to initiate the motion of such a polaron state accomplishing coherent long-range energy transfer along the steric structure of the helix protein matrix.

Based on physical arguments the coupled system can be cast into a form which makes it tractable for the exact construction of polaron states. More precisely, with view to the arrangement of the helix matrix one can assume that distortions of the hydrogen bonds from their rest alignments will be mainly oriented parallel to the  $z$  axis, i.e.  $s_{n,\mu} = z_{n,\mu} - z_{n-1,\mu}$ . Moreover, the predictably small deformations of the rigid covalent bonds may be discarded ( $r_{n,\mu} = 0$ ). In this way the vibrational degrees of freedom of the protein matrix are reduced to

one degree of freedom only, namely motions of the peptide group in the  $z$  direction leading to longitudinal stretchings and/or compressions of the hydrogen bonds. Additionally, for small distortions of the hydrogen bonds from their rest lengths we can expand the Morse potential. With the harmonic approximation  $U_{hyd}(s_{n,\mu}) = D(1 - e^{-as_{n,\mu}})^2 \approx a^2 D s_{n,\mu}^2$  the corresponding Hamiltonian is

$$\begin{aligned} H_{red} = H_{exc} + H_{vib} = & \sum_{n,\mu} \{(\epsilon_0 + \alpha_h(z_{n+1,\mu} + z_{n-1,\mu}))|c_{n,\mu}|^2 \\ & - (J_0 + \beta_h(z_{n+1,\mu} - z_{n,\mu})) [c_{n+1,\mu}^* c_{n,\mu} + c_{n+1,\mu} c_{n,\mu}^*] \\ & + L_0 [c_{n,\mu+1}^* c_{n,\mu} + c_{n,\mu+1} c_{n,\mu}^*] \} + \frac{1}{2m} \sum_{n,\mu} (p_{n,\mu}^{(z)})^2 + a^2 D \sum_{n,\mu} (z_{n,\mu} - z_{n-1,\mu})^2, \end{aligned} \quad (22)$$

from which we derive the following equations of motion for the *reduced* system:

$$\begin{aligned} i\dot{c}_{n,\mu} = & \alpha_h(z_{n+1,\mu} - z_{n-1,\mu})c_{n,\mu} - (c_{n+1,\mu} + c_{n-1,\mu}) + L_0(c_{n,\mu+1} + c_{n,\mu-1}) \\ & - \beta_h(z_{n+1,\mu} - z_{n,\mu})c_{n+1,\mu} - \beta_h(z_{n,\mu} - z_{n-1,\mu})c_{n-1,\mu}, \end{aligned} \quad (23)$$

$$\begin{aligned} \dot{p}_{n,\mu}^{(z)} = & (|c_{n+1,\mu}|^2 - |c_{n-1,\mu}|^2)\alpha_h - \beta_h [c_{n+1,\mu}^* c_{n,\mu} + c_{n+1,\mu} c_{n,\mu}^*] \\ & + \beta_h [c_{n,\mu}^* c_{n-1,\mu} + c_{n,\mu} c_{n-1,\mu}^*] - 2a^2 D(z_{n+1,\mu} - 2z_{n,\mu} + z_{n-1,\mu}), \end{aligned} \quad (24)$$

$$\dot{z}_{n,\mu} = p_{n,\mu}^{(z)}. \quad (25)$$

The system of equations (23)–(25) is hereafter referred to as the *reduced system*. Note that the terms related to the on-site energy  $\epsilon_0$  can be eliminated via the simple transformation  $c_{n,\mu}(t) \rightarrow e^{-i\epsilon_0 t} c_{n,\mu}(t)$ . In the limit case  $\beta_h = 0$  equations (23)–(25) recover the Davydov system [1].

Based on the fact that the velocity of the intermolecular transfer of excitonic energy is much lower than the velocity of sound of the acoustic bond vibrations it is justified to neglect the inertia in equation (24) [1, 11, 17]. As a consequence we can solve the resulting difference equations, the solution of which gives the (instantaneous) bond deformations

$$z_{n,\mu} - z_{n-1,\mu} = -\frac{\alpha_h}{2a^2 D} (|c_{n,\mu}|^2 + |c_{n-1,\mu}|^2) + \frac{\beta_h}{2a^2 D} (c_{n,\mu}^* c_{n-1,\mu} + c_{n,\mu} c_{n-1,\mu}^*). \quad (26)$$

Substitution of this expression in equation (23) yields a nonlinear discrete Schrödinger equation expressed in the excitonic amplitude:

$$\begin{aligned} i\dot{c}_{n,\mu} = & -\frac{\alpha_h}{2a^2 D} (|c_{n+1,\mu}|^2 + 2|c_{n,\mu}|^2 + |c_{n-1,\mu}|^2)c_{n,\mu} \\ & - (c_{n+1,\mu} + c_{n-1,\mu}) + L_0(c_{n,\mu+1} + c_{n,\mu-1}). \end{aligned} \quad (27)$$

Stationary localized solutions of equation (27) can be constructed with the help of a nonlinear map approach [33]. With the ansatz  $c_{n,\mu}(t) = \Phi_{n,\mu} e^{-iEt}$  the associated stationary equation is derived which is

$$\begin{aligned} E\Phi_{n,\mu} = & -\frac{\alpha_h}{2a^2 D} (|\Phi_{n+1,\mu}|^2 + 2|\Phi_{n,\mu}|^2 + |\Phi_{n-1,\mu}|^2)\Phi_{n,\mu} \\ & - (\Phi_{n+1,\mu} + \Phi_{n-1,\mu}) + L_0(\Phi_{n,\mu+1} + \Phi_{n,\mu-1}). \end{aligned} \quad (28)$$

This difference equation provides a nonlinear map

$$\{\Phi\} \rightarrow \{\Phi'\} = H\{\Phi\}/\|H\{\Phi\}\|, \quad (29)$$

the attractor of which represents the ground state of the excitonic system (for details see [33]). The operator  $H$  is determined by the rhs of equation (28) and the norm of the state  $H\{\Phi\}$  is defined as  $\|H\{\Phi\}\| = \sqrt{\sum_{n,\mu} (H\{\Phi\})^2}$ . We take a completely localized state  $\{\Phi_{n,\mu}\} = \delta_{n,n_0,\mu,\mu_0}$  as the initial condition for the map iteration and act on it with the operator



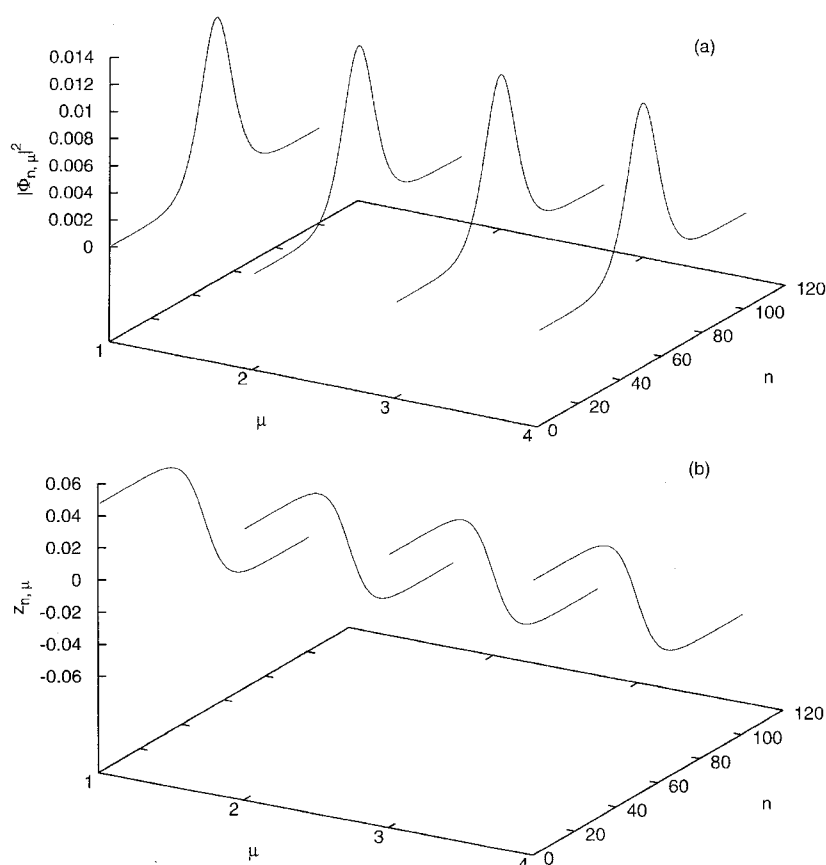


**Figure 1.** Profiles of the stationary polaron state  $\alpha$ -helix. Parameter  $\alpha_h = 2$ . (a) The excitonic pattern  $\Phi_{n,\mu}^2$ . (b) The static kink-like displacements  $z_{n,\mu}$  of the peptide groups.

*H*. The convergence is rapidly attained after a few iterations, yielding the excitonic component of the polaron. The associated static lattice deformations result then from equation (26).

In figure 1 (figure 2) we depict the polaron solution (localized excitonic state in companion with vibrational displacements localized in the same lattice region) of the  $\alpha$ -helix (3–10-helix) gained from the map. Both helix structures exhibit on each of their strands a localized excitonic contribution. The centre (maximum amplitude) of each amplitude distribution  $|c_{n,\mu}|^2$  is situated at the central lattice site (peptide group). In the case of the  $\alpha$ -helix the amplitudes decay exponentially and monotonically towards the ends of the strands, forming a single-hump solution. In contrast, in the case of the 3–10-helix one obtains an oscillating amplitude pattern in the form of a multi-hump solution for which the corresponding maxima become smaller the further its lattice position is away from the central site of a strand, so that the envelope of the amplitudes shows monotonic decay. Furthermore we observe that the exciton on the 3–10-helix is profoundly stronger localized than its counterpart on the  $\alpha$ -helix. Concerning the static distortions of the hydrogen bonds we note that the amplitude patterns of the displacements of the peptide groups in the  $z$  direction are characterized by kink-like structures. Accordingly, it holds that the further a H-bond is away from the left (right) of the central site the more compressed (stretched) it becomes. In comparison with the  $\alpha$ -helix system the deformations of the H-bonds for the 3–10-helix system are weaker (cf figures 1(b) and 2(b)).

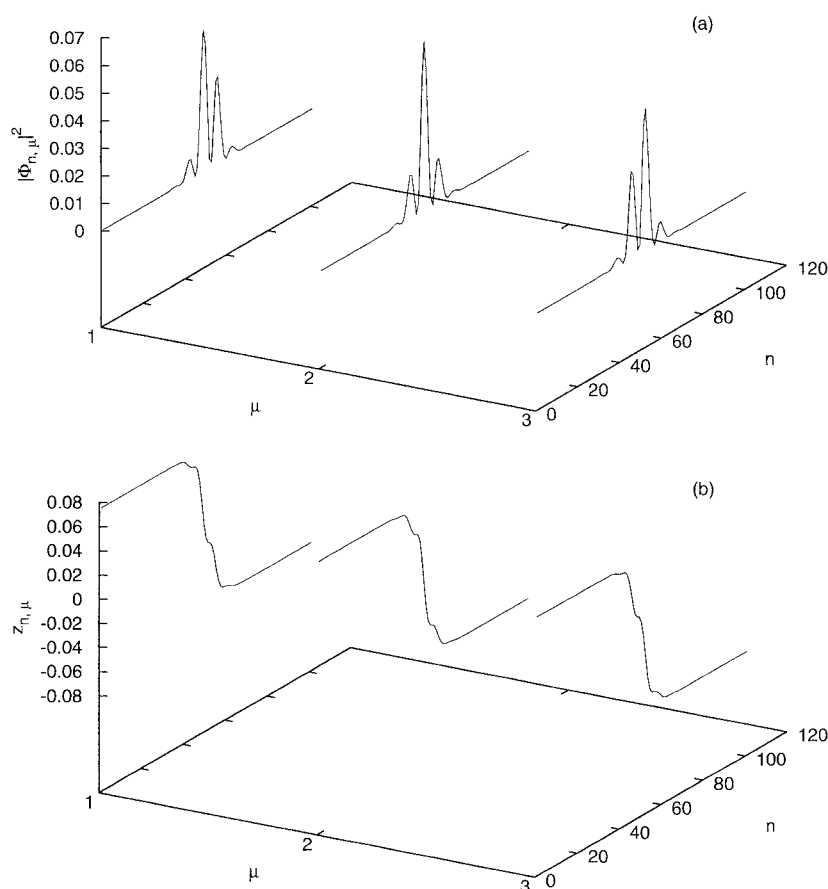


**Figure 2.** Profiles of the stationary polaron state of the 3–10-helix. Parameter  $\alpha_h = 2$ . (a) The excitonic pattern  $\Phi_{n,\mu}^2$ . (b) The static kink-like displacements  $z_{n,\mu}$  of the peptide groups.

Furthermore, with increased coupling strength  $\alpha_h$  the degree of localization is enhanced and a continuous transition from a large to a small polaron takes place on both helix structures. The size of the polaron plays a crucial role for its mobility. In fact, for large up to medium polarons coherent motion can be activated whereas small polarons are immobile due to their pinning to the discrete lattice [35, 36]. Additionally, for over-critical coupling strengths  $\alpha_h$  on the 3–10-helix one strand becomes distinguished in the sense that it contains the majority of the exciton energy. In other words the 3–10-helix then exhibits not only strong localization with respect to the  $n$  direction but also strong exponential concentration of the pulse on a single  $\mu$ -strand whereas for the  $\alpha$ -helix the symmetric excitation pattern of equal energy sharing between all the four strands is preserved.

#### 4. Exciton transfer mediated by mobile localized states

Before we embark on the investigation of the dynamics of the complete system we focus interest on the initiation of polaron motion in the reduced system given by equations (23)–(25) for which the polaron states can be exactly constructed using the map method. In order to

activate motion of the stationary localized exciton–vibron state (24) we utilize the pinning-mode method outlined in [37]. To this aim the pinning mode, as an internal localized polaron normal mode, has to be identified and subsequently implemented in the initial conditions for the integration of the dynamical system (for details see [37]). The pinning mode is obtained as a by-product of the stability analysis of the polaron solution. We performed the stability analysis in the standard manner, i.e. imposed small linear perturbations on the polaron solution, derived the corresponding tangent equations describing the evolution of these small perturbations and, eventually, constructed the Floquet map. In proving that all eigenvalues of the Floquet matrix lie on the unit circle in the complex plane we assured linear stability of the polarons for a wide range of the coupling parameter  $\alpha_h$ . Motion of the polaron is activated by a suitable perturbation of its momentum part  $\{p_{n,\mu}^{(z)}(t)\}$  in the direction of the associated pinning mode contribution  $\xi_{n,\mu}$ . The momentum component of the pinning mode, assigned to an isolated eigenvalue nearby the point  $(1, 0)$ , exhibits amplitude patterns with exponentially decaying envelopes symmetrically arranged around the central lattice site of each strand of hydrogen bonded peptide units. The initial conditions for the integration of the system (23)–(25) are chosen as follows:

$$\{\Phi_{n,\mu}, 0, z_{n,\mu}^{(0)}, 0\} + k\{0, 0, 0, \xi_{n,\mu}\}, \quad (30)$$

with the kick strength  $k$ . The numerical integration is performed with the help of a fourth-order Runge–Kutta scheme and the accuracy is checked by monitoring the conservation of the energy and the norm  $\sum_{n,\mu} |c_{n,\mu}(t)|^2$ . We imposed open boundary conditions simulating the fixed docking of the helix to the protein environment. Each strand of a helix consists of 101 peptide units. In figure 3 we depict the spatio-temporal evolution of the excitonic amplitudes  $|c_{n,\mu}(t)|^2$  on a single strand, illustrating the long-range coherent polaron motion. The polaron, i.e. the localized exciton in unison with its attributed displacement pattern  $z_{n,\mu}$ , propagates with uniform velocity along the lattice of peptide groups. We remark that there appear neither radial losses nor energy redistribution phenomena between the excitonic and the vibrational bond subsystems. Hence, the moving polaron retains its energy content for the  $\alpha$ -helix as well as 3–10-helix. During their journey along the peptide lattice the moving excitons change steadily their profile such that the localized structure is continuously shifted in the propagation direction under maintenance of the degree of localization.

## 5. Coherent exciton breather motion in the protein matrix

In this section we explore how the polaron solution of the reduced system reacts when the couplings to the full vibrations of the three-dimensional protein matrix are taken into account. For that reason the previously made assumptions, that the peptide groups experience deviations from their rest position exclusively in the  $z$  direction and that only the elastic hydrogen bonds get deformed along the helix axis, are abandoned and thus motion in all three dimensions is now possible. Consequently, distortions of the rather rigid covalent bonds as well as arbitrarily oriented deformations of the hydrogen bonds may occur. There arise at least two questions: do the polaron solutions of the reduced system persist as localized states of the complete system? If so, then we may ask: is the activation of their motion possible analogous to the procedure applied for the reduced system so that long-range coherent exciton transfer is established in a steric protein matrix too?

Since the polaron state of the reduced system does not establish an exact (ground state) solution of the full system we can expect that energy transfer processes between the excitonic and the bond vibrational subsystems take place. In the course of the energy migration the

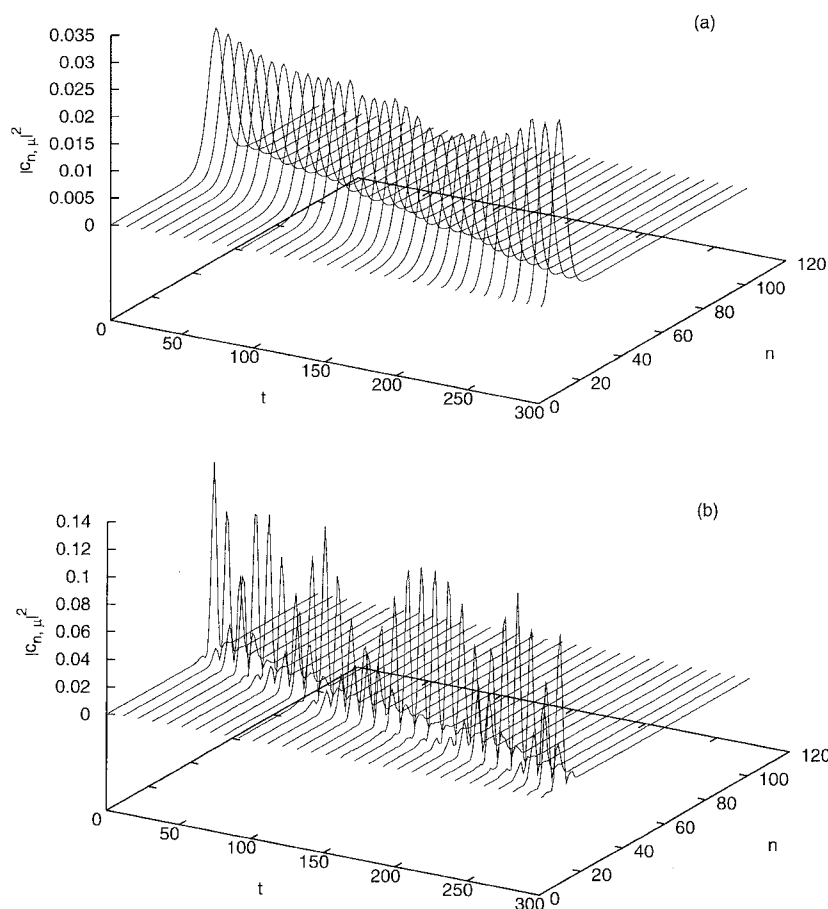


**Figure 3.** Coherent exciton transfer along a strand of hydrogen bonded peptide units of the helix. Motion is initiated by kicking the velocity  $\dot{z}_{n,\mu}$  initially along the direction of the pinning mode. Depicted is the amplitude profile of the excitonic amplitude  $|c_n(t)|^2$ . Parameter:  $\alpha_h = 3$ . (a) The  $\alpha$ -helix. (b) The 3–10-helix.

system might relax towards an equilibrium regime still supporting a stable localized exciton–vibron state.

First we investigate the adaptation behaviour of the polaron to its incorporation in the steric protein matrix of the  $\alpha$ - and 3–10-helix, respectively. We implemented the polaron of the reduced system as the initial condition in the full system. In figure 4 we illustrate the adaptation process for the excitonic component  $|c_{n,\mu}(t)|^2$  on a strand of the  $\alpha$ -helix and 3–10-helix, respectively. As the spatio-temporal patterns of the evolution of the exciton amplitude reveal the polarons respond quite differently to their vibrating cage environment, depending on the extension of the excitonic polaron pattern (degree of localization). On both helix forms the (original) static amplitude pattern develops into a breather, that is a spatially localized but time-periodic solution. Moreover, we observe that the stronger localized the polaron is the more pronounced is the energy exchange between the exciton and the vibrations of the steric protein matrix and the longer the relaxation phase lasts towards a balance of energy.

Interestingly, we found that for too strong a degree of (initial) localization the polaron is not adaptable to the steric protein matrix and rather decays in the course of time.

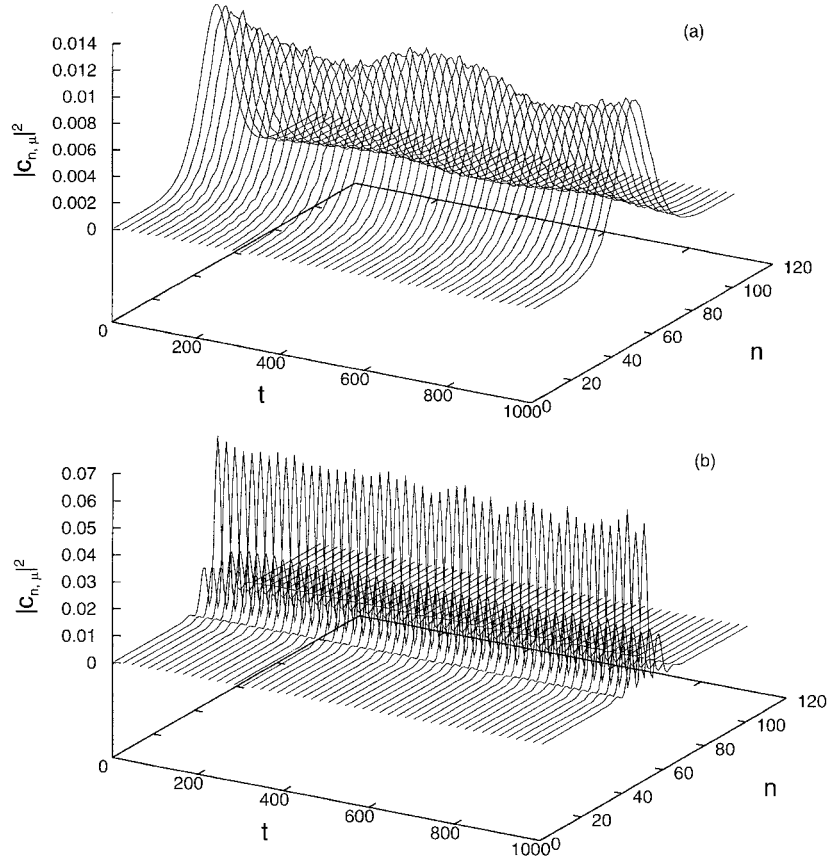


**Figure 4.** The adaptation of the excitonic component of the (original) static polaron into an exciton breather. Shown is the spatio-temporal evolution of the exciton pattern on a single strand. (a) The  $\alpha$ -helix. (b) The 3–10-helix.

For a quantitative assessment of the energy sharing phenomena related to the relaxation process we consider the interaction energy of the exciton and the vibrations of the protein matrix. To this end we divide the Hamiltonian associated with the exciton dynamics into two parts:  $H_{exc} = H_p + H_{int}$ . The part  $H_p$  includes the pure excitonic energy

$$H_p = \sum_{n,\mu} \{-J_0[c_{n+1,\mu}^* c_{n,\mu} + c_{n+1,\mu} c_{n,\mu}^*] + L_0[c_{n,\mu+1}^* c_{n,\mu} + c_{n,\mu+1} c_{n,\mu}^*]\}, \quad (31)$$

while the remaining part  $H_{int}$  describes the dynamical modulations of the excitonic parameters through vibrations of the protein matrix:

$$\begin{aligned} H_{int} = & \sum_{n,\mu} \{[\alpha_c(r_{n,\mu+1} + r_{n,\mu}) + \alpha_h(s_{n+1,\mu} + s_{n,\mu})]|c_{n,\mu}|^2\} \\ & - \sum_{n,\mu} \{\beta_h s_{n+1,\mu} [c_{n+1,\mu}^* c_{n,\mu} + c_{n+1,\mu} c_{n,\mu}^*]\} \\ & + \sum_{n,\mu} \{\beta_c r_{n,\mu+1} [c_{n,\mu+1}^* c_{n,\mu} + c_{n,\mu+1} c_{n,\mu}^*]\}. \end{aligned} \quad (32)$$

From the temporal evolution of the exchange energy  $H_{int}$ , depicted in figure 5, one can infer the state of the energy redistribution between the exciton and the protein matrix. In the case of

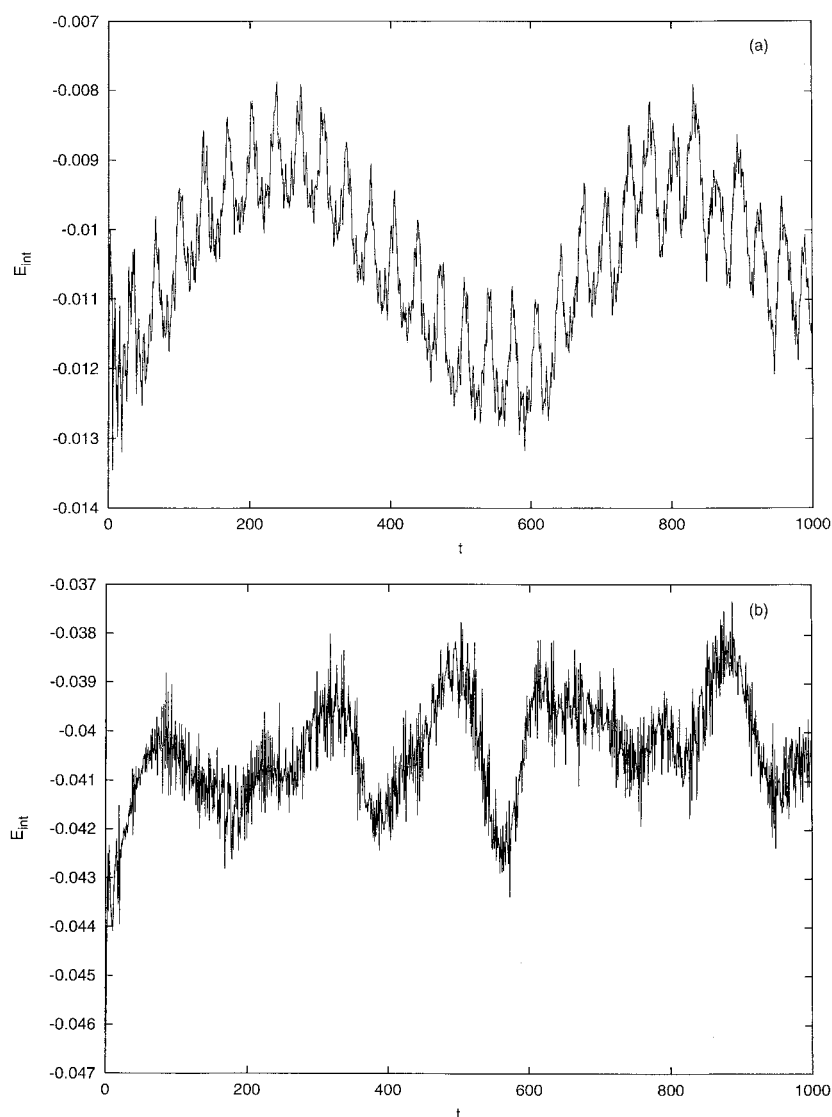


**Figure 5.** Time evolution of the interaction energy  $H_{int}$  defined in equation (32). Parameter  $\alpha_h = 2$ . (a) The  $\alpha$ -helix. (b) The 3–10-helix.

the 3–10-helix the adaptation of the polaron to the protein cage proceeds in a relatively long phase of about 200 time units ( $\simeq 140$  ps) during which  $H_{int}$  grows, on average. Afterwards an equilibrium regime is reached characterized by little and almost periodic modifications of  $H_{int}$  with maximal deviations of the order of 7% from the mean value. However, in the case of the  $\alpha$ -helix it takes shorter times ( $\approx 20$  time units) to approach the stationary regime when the average amplitude of  $H_{int}$  oscillates with maximal excursions of 10% from the mean value.

Generally, as far as the bond deformations are concerned we observe that, in the course of the relaxation process, energy gets redistributed into extended parts of the protein matrix. Eventually, (almost) all covalent bonds get distorted from their rest lengths. However, these

bond distortions are the weaker the more the corresponding region of the helix is apart from the main excitation centre where the polaron has been launched. Consequently, a localized structure in the covalent bond distortion profile in the form of a phonobreather [38] has been created. With regard to the hydrogen bonds we observe a similar result in the outcome of the relaxation dynamics, i.e. some amount of energy flows into the hydrogen bonds being distant from the excitation centre but the deformations stay mainly localized around the exciton centre besides the extended tail. Most importantly the localized shape of the excitonic amplitude profile is maintained too. Hence, the new equilibrium state formed exhibits a localized structure, being reminiscent of those associated with the polaron state of the reduced system. In summary, comparing the adaptation process for the two different helix forms we note that for the  $\alpha$ -helix the adaptation of the polaron to the protein cage proceeds faster than for the 3–10-helix and in the latter case the energy exchange between the polaron and the steric protein cage is more pronounced than in the former case, leading to the conclusion that the  $\alpha$ -polaron is more adaptable than the 3–10 one.

As an attempt to initiate exciton transfer within the steric geometry of the protein matrix we imposed again the momentum component of the pinning mode of the reduced system to the initial conditions for the full system. In order to ensure that the polarons possess (at least initially) comparable localization properties for both helices we adjusted the coupling parameter  $\alpha_h$  for the  $\alpha$ -helix accordingly. Interestingly, coherent long-range exciton motion is achievable in both helix systems. We obtain moving localized excitonic pulses. Except for the breathing amplitudes the character of the motion in the full system, realized by moving exciton breathers, is qualitatively the same as the for the travelling excitonic polaron component in the reduced system. In particular, the breathers travel with uniform velocity. The exciton breather on the  $\alpha$ -helix moves with higher velocity than the one on the 3–10-helix. The breather motion in the full system is connected with a small and periodic energy exchange between the excitonic and the bond vibration subsystems.

## 6. Summary

This paper was devoted to a study of the transfer of vibronic energy (quanta of amide-I vibrations) in helical proteins. The steric structure of the helix protein was described in terms of a three-dimensional oscillator network for which each constituent represents a peptide group which can perform genuine three-dimensional motions contributing to deformations of the adjacent covalent and hydrogen bonds within the protein matrix. The bond forces were modelled by pair–pair interactions. We considered the two most common helix forms of proteins, namely  $\alpha$ -helices and 3–10-helices. The propagation of vibronic amide-I energy was described as exciton hopping across the peptide groups in the context of a tight-binding system. Coupling between the excitonic degree of freedom and the bond vibrations arose from a dependence of the excitonic parameters (on-site energy and hopping integrals) on the distortions of the bonds from their equilibrium lengths allowing for the exchange between excitonic and vibrational energy. In the first part of the paper we considered a reduced system by assuming that the soft hydrogen bonds get deformed parallel to the helix axis only. Additionally, distortions of the rigid covalent bonds were discarded. For the reduced system polaron solutions consisting of a localized exciton and the attributed localized lattice deformations (local deformations of the hydrogen bonds) were constructed exactly on the basis of a nonlinear map approach. The pinning-mode concept was applied to activate polaron motion, establishing coherent long-range exciton transfer along the peptide units of the protein matrix.

In the second part of the paper we paid attention to the adaptation process taking place when the polaron of the reduced system is incorporated into the full vibrational dynamics of the protein matrix including deformations of the covalent bonds as well as of the hydrogen bonds not necessarily aligned along the helix axis. In course of the relaxation dynamics we observed that exchange of energy between the exciton and the bond vibrational system takes place. In particular, due to the directed flow of energy into the covalent bonds they experience (small) deformations. However, regarding their contributions to the distortions of the protein cage from the rest configuration they play a minor role opposed to the distortions of the soft hydrogen bonds. Eventually, the energy redistribution into the bond system terminates and the coupled dynamics relaxes onto a new equilibrium regime exhibiting a breather-like excitation pattern. The excitonic component of the polaron proved to be robust throughout the relaxation process and maintained its localized shape and the majority of its energy content representing such a stable localized exciton solution of the full protein matrix system. The lattice of the covalent and the hydrogen bonds supports phonobreaters. Interestingly, coherent motion of these exciton breathers can be initiated through proper injection of kinetic energy providing the long-range transfer of amide-I energy in the steric protein cage. Regarding the effect of the helix geometry we note that the polaron on the  $\alpha$ -helix adapts in shorter times to the couplings to the vibrations of the full protein cage with which it exchanges less energy compared to the polaron of the 3–10-helix. In addition, the exciton breather on the  $\alpha$ -helix moves with higher velocity than the one on the 3–10-helix so that we could draw the conclusion that an  $\alpha$ -helix provides the better medium for vibronic energy transfer. The fact that the  $\alpha$ -helix form of proteins is more common than any other helical protein structure reflects the selectivity and efficiency of the formation process of different protein structures being of importance for their biological functions.

### Acknowledgment

One of the authors (DH) acknowledges support by the Deutsche Forschungsgemeinschaft via the Heisenberg program (He 3049/1-1).

### References

- [1] Davydov A S 1973 *J. Theor. Biol.* **38** 559  
Davydov A S and Kislukha N I 1976 *Sov. Phys.–JETP* **44** 571  
Davydov A S 1982 *Sov. Phys.–Rev.* **B 25** 898
- [2] Davydov A S 1985 *Solitons in Molecular Systems* (Dordrecht: Reidel)  
Davydov A S 1973 *J. Theor. Biol.* **38** 559
- [3] Scott A C 1981 *Phys. Lett. A* **86** 60
- [4] Hyman J M, McLaughlin D W and Scott A C 1981 *Physica D* **3** 23
- [5] Scott A C 1982 *Phys. Rev. A* **26** 578  
Scott A C 1983 *Phys. Rev. A* **27** 2767
- [6] Scott A C 1982 *Phys. Scr.* **25** 651  
Scott A C 1984 *Phys. Scr.* **29** 279
- [7] Eilbeck J C, Lomdahl P S and Scott A C 1984 *Phys. Rev. B* **30** 4703
- [8] Brown D, West B J and Lindenberg K 1986 *Phys. Rev. A* **33** 4104  
Brown D, West B J and Lindenberg K 1986 *Phys. Rev. A* **33** 4110
- [9] Ivic Z and Brown D 1989 *Phys. Rev. Lett.* **63** 426
- [10] Christiansen P L and Scott A C (ed) 1990 *Self-Trapping of Vibrational Energy* (New York: Plenum)
- [11] Scott A C 1992 *Phys. Rep.* **217** 1
- [12] Cruzeiro-Hansson L 1992 *Phys. Rev. A* **45** 4111  
Cruzeiro-Hansson L 1994 *Phys. Rev. Lett.* **73** 2927
- [13] Förner W 1991 *Phys. Rev. A* **44** 2694



- Förner W 1991 *J. Phys.: Condens. Matter* **3** 1915  
Förner W 1992 *J. Phys.: Condens. Matter* **4** 4333  
Förner W 1993 *J. Phys.: Condens. Matter* **5** 3897
- [14] Christiansen P L and Scott A C (ed) 1991 *Davydov's Soliton Revisited* (New York: Plenum)
- [15] Peyrard M (ed) 1995 *Proc. Int. School Nonlinear Excitations in Biomolecules (Les Houches Session 1994)* (Berlin: Springer)
- [16] Zolotaryuk A V, Spatschek K H and Savin A V 1996 *Phys. Rev. B* **54** 266
- [17] Kundu K 2000 *Phys. Rev. E* **61** 5839
- [18] Cruzeiro-Hansson L, Eilbeck J C, Marin J L and Russell F M 2000 *Phys. Lett. A* **266** 160
- [19] Gheorghiu-Swirschevski S 2001 *Phys. Rev. E* **64** 051907
- [20] Zolotaryuk Y and Eilbeck J C 2001 *Phys. Rev. B* **63** 054302-1
- [21] Xie A, van der Meer L, Hoff W and Austin R H 2000 *Phys. Rev. Lett.* **84** 5435
- [22] Hamm P, Lim M and Hochstrasser R M 1998 *J. Phys. Chem. B* **102** 6123
- [23] Edler J and Hamm P 2002 *J. Chem. Phys.* **117** 2415
- [24] Branden C and Tooze J 1991 *Introduction to Protein Structure* (New York: Garland)
- [25] McCammon J A and Harvey S C 1987 *Dynamics of Proteins and Nucleic Acids* (Cambridge: Cambridge University Press)
- [26] Olsen O H, Samuelsen M R, Petersen S B and Nørskov L 1988 *Phys. Rev. A* **38** 5856
- [27] La Magna A, Pucci R, Piccitto G and Siringo F 1995 *Phys. Rev. B* **52** 15273
- [28] Zolotaryuk A V, Christiansen P L and Savin A V 1996 *Phys. Rev. E* **54** 3881
- [29] Christiansen P L, Zolotaryuk A V and Savin A V 1997 *Phys. Rev. E* **56** 877
- [30] Voulgarakis N K, Hennig D, Gabriel H and Tsironis G P 2001 *J. Phys.: Condens. Matter* **13** 9821
- [31] Hennig D 2001 *Phys. Rev. E* **64** 041908-1
- [32] Hennig D 2002 *Phys. Rev. B* **65** 174302
- [33] Kalosakas G, Aubry S and Tsironis G P 1998 *Phys. Rev. B* **58** 3094
- [34] Voulgarakis N K and Tsironis G P 2001 *Phys. Rev. B* **63** 14302
- [35] Peyrard M and Kruskal M D 1984 *Physica D* **14** 88
- [36] Flach S and Willis C R 1998 *Phys. Rep.* **295** 181
- [37] Chen D, Aubry S and Tsironis G P 1996 *Phys. Rev. Lett.* **77** 4776
- [38] Aubry S 1997 *Physica D* **103** 201